Response to Referee #1:

We would like to express our sincere gratitude to Professor Horvath for his helpful comments that will contribute to improve the quality of the manuscript. A point by point response is included below. Comments are in blue and italics, and our responses are in black.

Titos et al. have analyzed a large set of data with respect to humidity growth. The work horse for this investigation are two nephelometers operating at <40% RH and at high relative humidity. As can be seen from figure 7 there is a slight decrease in scattering coefficient for humidity below 40%, thus a precise value of the reference humidity is needed. I miss a description of the method. If the low humidity is achieved by temperature increase some volatile parts of the aerosol particles might disappear, which on the other hand are included in the wet nephelometer. If diffusion drying is used, the same argument applies. So a description of the drying process and a discussion of possible effects of artefacts is needed. (page 3366 lines 6 to 7)

The measurements presented in this study were conducted following the standard aerosol sampling protocol of the GAW network. The sampled aerosol was gently heated when necessary to achieve a low relative humidity (RH) of 40% or below. The mean ± standard deviation of the temperature and relative humidity within the dry nephelometer for the whole measurement campaign were T = 26±4 ºC and RH = 30±13 %. In order to minimize losses of volatile compounds the temperature of the sampled air was kept below 35 ºC (Bergin et al., 1997; ten Brink et al., 2000). Only 0.5% of the 1-min observations occurred at temperatures above this value and these data were not further considered in the study. Despite these considerations, if losses of volatile compounds occurred due to heating, both nephelometers would be affected since the nephelometers were operated in series separated by the humidifier control system. This information and the corresponding references will be included in the Instrumentation section of the revised manuscript.

Bergin, M. H., J. A. Ogren, S. E. Schwartz, and L. M. McInnes. 1997. Evaporation of ammonium nitrate aerosol in a heated nephelometer: Implications for field measurements. Environ. Sci. Technol., 31, 2878–2883.

ten Brink, H. M., A. Khlystov, G. P. A. Kos, T. Tuch, C. Roth, and W. Kreyling. 2000. A high flow humidograph for testing the water uptake by ambient aerosol. Atmos. Environ., 34, 4291–4300.

The scattering enhancement factor with respect to wind speed is indirectly biased by the direction, since in this investigation lower wind speed also means winds from the West, which is evident in figure 6. So I suggest to omit the right part of figure 5, since the better information is given in figure 6.

Following the reviewer suggestion we have omitted Figure 5, since the better information is given in Figure 6 and this figure is also easier to visualize. Figures have been renumbered accordingly.

It is difficult to guess the humidity growth with only one information on the aerosol (the single scattering albedo). The authors are aware of this and the large error bars on the first constant in equation 4 and 5 demonstrate this, which even make it likely that no increase in scattering coefficient can occur. This relation obtained by the authors mainly has been found since only two types of aerosols are "competing": Sea salt particles on the one hand, and the high influence of the anthropogenic aerosols on the other hand. If a third component, e.g. desert aerosol particles could also occur, this formula may fail.

We agree with Prof. Horvath in that the parameterization has limitations. We are aware that this particular study had a strong covariance between SSA and SAE, which allowed a reduction in the γ fit to a single parameter and that this relationship is only valid for the TCAP data. In this particular study, the coarse mode was predominantly dominated by sea salt particles and the presence of other species that typically accumulate in the coarse fraction like dust particles was negligible. Due to the similar characteristics of sea salt and dust particles in terms of SAE and SSA, but the strong difference in the hygroscopic behavior, the parameterization proposed in this study would fail under the presence of both types of aerosols as dust does not experience significant hygroscopic growth. The Cape Cod study may be considered as representative of an aerosol from the Northern Atlantic coast with anthropogenic influence. The same analysis needs to be applied to other regions and aerosol types to catalog exponential fit parameters of γ versus SSA over a variety of aerosol types and atmospheric conditions. In this sense, preliminary analysis to check the validity of this parameterization at different sites (pristine and polluted marine, anthropogenic, rural, desert and forest sites) suggest that the model agrees well with the experimental measurements for all sites except for the desert site (Titos et al., 2014). The discussion about the limitations of the parameterization will be strengthened in the revised manuscript.

Titos, G., Jefferson, A., Sheridan, P. J., Andrews, E., Lyamani, H., Ogren, J. A. and Alados-Arboledas, L.: Estimating aerosol light-scattering enhancement from dry aerosol optical properties at different sites, European Geoscience Union Assembly, Vienna, 2014.

Response to Referee #2:

We would like to express our sincere gratitude to the anonymous referee for his/her helpful comments that will help to improve the quality of the manuscript. A point by point response is included below. Comments are in blue and italics, and our responses are in black.

Titos and coauthors for publication in Atmospheric Chemistry Physics.

The authors have used data collected by the aerosol observing system during the Two Column Aerosol Project to characterize the aerosol characteristics at Cape Cod, MA. The authors have reported the observed aerosol light-absorption and light-scattering coefficients together with the single scattering albedo and Angstrom exponent. The scattering enhancement factor is also calculated by using the observations from the dry and wet nephelometers. The authors have proposed an exponential equation that estimates aerosol hygroscopic growth as a function of single scattering albedo. I think the article is well-written and will be of use to scientist studying aerosol radiative properties together with the wider meteorological community. But I see that the article falls short in some ways and hence recommend it to be published after major revisions. Please find below my specific comments.

Major Comments:

1) During the TCAP field campaign there were two aerosol observing systems part of the AMF-1, the aerosol observing system (AOS) and Marine aerosol observing system (MAOS). The article should use the data from the condensation particle counter (CPC) and the Hygroscopic Tandem Differential Mobility Analyzed (HTDMA), part of the MAOS and AOS to characterize the aerosol size distribution and size increase due to increase in RH.

This is a really good suggestion. However, as far as we know, the MAOS data is not yet available for distribution. The current data in the ARM archive are raw data with no flow, dilution and inversion corrections to the data. In addition, the two sets of measurements overlapped for only one month. For these reasons, we are unable to compare the two data sets.

2) The authors have done a good job in summarizing the aerosol radiative properties as measured by the AOS. But the article falls short in describing the general meteorology during the presence of the aerosols. Mainly, a plume of aerosols might be coming from an urban area, but if precipitation is accompanied by that plume, then due to aerosol scavenging, the number concentration will be less and so will be the aerosol impact on atmospheric radiation. So, I highly encourage the authors to include some description of the meteorological conditions during the presence of different aerosol composition.

Following the referee suggestion, we will include a paragraph summarizing the mean meteorological features during the campaign in the Overview section of the revised manuscript and in the wind sector analysis section to emphasize the different meteorological features during the presence of different aerosol types. Concerning the effect of precipitation, we agree with the referee in the importance of precipitation in the measured aerosol properties. Precipitation will have an effect not only on the total scattering but on the aerosol size distribution and composition. To reduce the influence of instrument noise on the γ calculation, low scattering events (which are normally associated with precipitation) were excluded from the data analysis (only values of σ_{sp}(550 nm) > 5 Mm^{-1} were considered). Trying to correlate the aerosol hygroscopic growth to precipitation would be difficult as most of those data were excluded from the analysis. For a comprehensive analysis we would need to include precipitation events not only at the immediate site, but also several hours downwind of the site. This type of work is beyond the scope of this paper, which focuses mainly on the development of a new empirical method for estimating aerosol hygroscopic growth.

3) From the AOS and MAOS data, in addition to the quantities calculated by the authors, it is also possible to calculate the backscatter fraction and submicron scattering fraction. Calculation of these quantities might (probably) provide some insights on the aerosol composition. Fan et al. (2010 JGR) and Manoharan et al. (2014 ACP) might be of some help.

We agree with the reviewer in that interesting information can be derived from the backscatter fraction and the submicron scattering fraction. Thus, we will include these variables in the revised manuscript.

4) The authors have described the figures in the text, but many a times have not drawn any scientific conclusions from them or at least speculated the scientific importance of the data. For example, I am not sure what scientific insights are gained from Fig 3. I suggest the authors go through the manuscript and figures again and draw some science conclusion from the presented data. Thanks.

We have changed the wording on page 3370 - line 14 to better clarify the intent of Figure 3. The graph shows that for situations dominated by aerosol sea salt (SAE<1) the scattering in the PM_1 fraction experienced a higher enhancement than in the PM_{10} fraction. This indicates that small sea salt particles have a larger scattering enhancement compared to coarse sea salt particles. This behavior can be explained by a shift in the size distribution to a scattering regime with a higher scattering efficiency when the SAE is greater than 1. This information will be included in the revised manuscript.

We have strengthened the discussion of Figure 4 in order to clarify the main scientific features of it. Furthermore, as recommended by Prof. Horvath in his review, we have

omitted Figure 5, since the better information is given in Figure 6 and this figure is also easier to visualize than Figure 5. Figures have been renumbered accordingly.

5) The Cimel sun-photometer and Multi-Filter Rotating Shadowband Radiometer (MFRSR) are also part of the AMF-1 and measure the aerosol optical depth (AOD). It will be great if the authors also characterize the AOD measurements.

We agree with the referee that including the results derived from CIMEL measurements might be interesting. However, we believe that it does not add to the content of this paper and to the analysis of the scattering enhancement due to water uptake that is the main objective of the work. Comparison of the data with AOD is beyond the scope of this paper as it requires information on the meteorological variables and aerosol particles properties with vertical resolution.

Minor Comments:

1) Line 3-4 page 3362: I am not sure TCAP is some kind of framework, it was a ARM funded field campaign. Please revise the sentence to reflect that.

We have corrected it throughout the text.

2) Line 10 page 3366: PTFE stands for Polytetrafluouroethylene … it will be great if you mention the full-form of PTFE together with PTFE.

Done.

3) Section 2.1: While describing AMF-1 instrumentation, usually the article Mather and Voyles (2013, BAMS) and Miller and Slingo (2007, BAMS) are mentioned.

The aforementioned references will be included.

4) Page 3368, Line 7: Not sure what the "de" is after 550 nm.

We apologize for the mistake; this was a typo that will be corrected in the revised version of the manuscript.

5) The measured quantities are absorption and scattering coefficients. You have provided equations for SAE and f(RH,λ), but have not done so for SSA. It will be great if you do that too.

We will explicitly include the equation for calculating SSA in the revised manuscript. Due to the inclusion of the backscatter and the submicron scattering fractions in the revised manuscript, the equations needed for their calculation will be also included in the Methodology section.

Response to Paul Zieger:

We would like to thank Dr. Zieger for the useful comments. We have responded to each specific comment in detail and will update the manuscript according to his suggestions, which we believe has helped to strengthen and clarify the study. Comments are in blue and italics, and our responses are in black.

Titos et al. present and discuss in their manuscript the results of a measurement campaign at Cape Cod, Massachusetts, where aerosol optical measurements were measured for one year. The focus is the scattering enhancement factor f(RH) which is defined as the aerosol particle scattering coefficient at enhanced relative humidity (RH) divided by its dry value. This parameter was measured by a humidified nephelometer system for approx. 7 months within this year. f(RH) was analysed with regard to air mass origin and compared to other aerosol optical parameters like the single scattering albedo (SSA) and Ångström parameter. A parametrization is being proposed which allows estimation of f(RH) using the SSA as a proxy.

I have read this paper with great interest and would like to share some comments (and questions) to further improve the quality of this manuscript:

• The authors use a two-parameter equation to parametrize the measured humidograms of f(RH), but focus only on the discussion of the γ parameter and ignore the intercept a. How did it vary for the different air masses? I would guess that a > 1 during sea salt periods, or? Looking at Fig. 7, I have the impression that all measured humidograms are slightly biased towards larger values at low RH (where it should, ideally, reach 1). Could this be an effect of the slight disagreement between the two nephelometers at dry conditions?

The "a" parameter was used to recalculate f(RH) values measured at different RH to RH=80% using equation 3 (equation 6 in the revised manuscript). The focus was kept in the γ parameter since it parameterizes the magnitude of the scattering enhancement, which is the main objective of this study. Performing the fitting for RH>40%, a mean value of a = 0.85±0.15 for the whole campaign was obtained, which is in agreement with the value of a = 0.9±0.1 reported by Zieger et al. (2014). The "a" parameter varies with the aerosol transmission efficiency through the humidifier and goodness of the power law fit. Note also that slight differences between the experimental and ideal value of "a" are expected since the "a" value will depend also on aerosol losses in the dry nephelometer and in the humidifier system.

Zieger, P., R. Fierz-Schmidhauser, L. Poulain, T. Müller, W. Birmili, G. Spindler, A. Wiedensohler, U. Baltensperger, and E. Weingartner. 2014. Influence of water uptake on the aerosol particle light scattering coefficients of the Central European aerosol. Tellus B, 66, 22716, http://dx.doi.org/10.3402/tellusb.v66.22716.

• Page 3367, Line 4: Was the difference between the two nephelometers accounted for when calculating f(RH)? Could the authors speculate on why the agreement is much better for PM1 compared to the PM10?

No, the difference was not accounted when calculating f(RH). The difference between both nephelometers might be ascribed to sampling losses in the dry nephelometer and in the humidifier system. Many authors correct the humidified nephelometer measurements by applying an empirical correction factor (the slope of the regression between dry and humidified nephelometers). This correction factor will not affect the gamma parameter which is the main objective of this work but it will modify the "a" parameter. In any case, we would not say that the agreement was much better for PM_1 than for PM_{10}. The slope of the regression was 0.971±0.004 for PM_1 and 1.073±0.001 for PM_{10} but the intercepts differ also for each size fraction. When fitting through zero, the differences between both slopes were lower than 4%. In addition, there are much data dispersion for PM_1 (R^2 = 0.77) than for PM_{10} (R^2=0.99).

• If I am correct, it should be mentioned in the revised manuscript that the applied humidified nephelometer set-up will only capture the lower branch of the hysteresis curve and will miss the upper branch because no active drying (keeping the humidifier on maximum) is performed before the particles reach the second nephelometer (see Fierz-Schmidhauser et al., 2010).

We agree with Dr. Zieger in that our humidified nephelometer system can only capture the lower branch of the hysteresis curve. We will include this information in the revised manuscript.

• Page 3370, Line 24 and Sect. 4.2: We have made an interesting observation in the Arctic (Zieger et al., 2010) of compensating effects between size and aerosol hygroscopicity. At the beginning of the campaign we had mainly small and less hygroscopic particles compared to the end where large but more hygroscopic particles (mainly sea salt) led to the same magnitude of f(RH). Can this maybe also be seen in your data set, when e.g. comparing size distribution parameters to f(RH)?

We observed that when small anthropogenic particles predominated (large SAE values) the particles were less hygroscopic while when coarse particles predominated (small SAE values) the particles were more hygroscopic and the results suggest that the aerosol was dominated by sea salt particles (see Figures 8 and 9). Thus, γ decreased as the SAE increased (the correlation coefficient of γ versus SAE was R = -0.77). This result contrasts with the result of Zieger et al. (2010) that showed a decrease of γ for an increase in the contribution of coarse particles, probably connected with the compensating effects between different varying aerosol properties discussed in their work. This information and the corresponding reference will be included in the revised manuscript.

The interesting observation in our study is that we took advantage of the size segregated f(RH) data and we found that fine sea salt particles were more hygroscopic than coarse sea salt particles (see Figure 3 of the manuscript). This could be due to the large increase in f(RH) of NaCl with decreasing particle size as Zieger et al. (2013) also showed. On the other hand, this behavior might be also due to a shift in the size distribution to a scattering regime with a higher scattering efficiency when the SAE is greater than 1. We have strengthened the discussion of Figure 3 in order to include this information.

• Page 3371, first paragraph: A nice way of showing the influence of sea spray on the deliquescence could be to plot $\mu = 1 - \gamma_{<65\%}/\gamma_{>75\%}$ *vs. a size distribution parameter (see Fig. 8 and Eq. 9 in Zieger et al., 2010). In the Arctic these parameters were clearly correlated.*

In our case, the hysteresis index as introduced in Zieger et al. (2010) did not correlate with the scattering Ångström exponent neither with the sub-micrometer scattering factor, $R_{sp}(\lambda) = \sigma_{sp(Dp < 1\ \mu m)}(\lambda)/\ \sigma_{sp(Dp < 10\ \mu m)}(\lambda)$. Due to the lack of correlation, we did not introduce the hysteresis index and discuss it in the manuscript.

• Sect. 4.4: I think the limitations of the proposed parametrization should be further discussed. It might be true that a simple site-specific proxy can be found to predict f(RH) at Cape Cod, but the same proxy can fail for another (even marine) site. We have done a sensitivity analysis to exactly address this question (see Sect. 6.3 in Zieger et al, 2013) because it was not possible to find one simple parametrization for all different analysed aerosol types. A reliable prediction, especially for climate models, will always need a full determination of the particle number size distribution (fine and coarse mode) and information on the chemical composition or particle hygroscopicity.

We agree with Dr. Zieger in that for a reliable prediction of the aerosol scattering enhancement using Mie theory, the particle number size distribution and the chemical composition are needed. However, that approach also has some disadvantages. For example, for predicting f(RH) using Mie theory, strong assumptions are usually made like spherical and homogenous internally mixed particles, constant refractive index, etc., which led to an overall relative uncertainty in the calculated f(RH) up to 25 % as reported in Zieger et al. (2013). In addition, at least two instruments are needed for measuring the whole size distribution plus instrumentation to measure the chemical composition. This set-up is not as common as it would be desirable, so the global coverage is reduced by using these measurements.

Using the single scattering albedo and/or scattering Angström exponent as estimators for the f(RH) has the advantage that those measurements are widely performed in GAW and ACTRIS networks. However, we agree that the parameterization has limitations. We are aware that this particular study had a strong covariance between SSA and SAE, which allowed a reduction in the γ fit to a single parameter and that this relationship is only valid for the TCAP data. In this particular study, the coarse mode was predominantly dominated by sea salt particles and the presence of other species that typically accumulate in the coarse fraction like dust particles was negligible. Due to the similar characteristics of sea salt and dust particles in terms of SAE and SSA, but strong difference in the hygroscopic behavior, the parameterization proposed in this study would fail under the presence of both types of aerosols as dust does not experience significant hygroscopic growth. Cape Cod may be considered as representative of an aerosol from the Northern Atlantic coast with anthropogenic influence. The same analysis needs to be applied to other regions and aerosol types to catalog exponential fit parameters of γ versus SSA over a variety of aerosol types and atmospheric conditions. In this sense, preliminary analysis to check the validity of this parameterization at different sites (pristine and polluted marine, anthropogenic, rural, desert and forest sites) suggest that the model agrees well with the experimental measurements for

all sites except for the desert site (Titos et al., 2014). The limitations of the proposed parameterization will be further discussed in the revised manuscript.

Titos, G., Jefferson, A., Sheridan, P. J., Andrews, E., Lyamani, H., Ogren, J. A. and Alados-Arboledas, L.: Estimating aerosol light-scattering enhancement from dry aerosol optical properties at different sites, European Geoscience Union Assembly, Vienna, 2014.

• How should a be treated within the proposed parametrization?

The parameter "a" is not included in the parameterization so the equation proposed can be used to estimate the γ parameter but not "a". The "a" parameter would act as a normalization factor but the scattering enhancement characterized by the γ parameter will not be affected.

• Page 3363, Line 17: The authors should also mention recent studies of Zieger et al. (2011, 2012) where humidified nephelometer measurements were explicitly performed to validate or compare remote sensing measurements of the aerosol extinction coefficient with in-situ measurements at ambient conditions.

We will include the aforementioned references.

• Page 3364, Line 11: The longest campaign was actually 4 months long (Cabauw).

We apologize for the mistake; 3 months will be replaced by 4 months in the revised manuscript.

• Fierz-Schmidhauser et al. (2010) also performed PM10 and PM1 measurements of f(RH) (actually together with the humidograph system of DOE/ARM).

We will include the reference in the revised manuscript although the intention here was only to mention a few examples of papers that reported scattering enhancement factors in PM_1 and PM_{10}. The paper of Fierz-Schmidhauser et al. (2010) was not initially listed here because the paper is mainly focused on the comparison of both humidifier systems and not in the characterization of aerosol hygroscopicity in PM_{10} and PM_1 size fractions.

• Page 3366, Line 7: Could you state the mean and standard deviation of temperature and relative humidity within the dry nephelometer?

The mean ± standard deviation of the temperature and relative humidity within the dry nephelometer for the whole measurement campaign were T = 26±4 ºC and RH = 30±13 %. It is important to note that, as stated in Page 3368-line 21, for the calculation of f(RH) and γ parameter only cases when the RH inside the dry nephelometer was below 40% were used. This information will be included in the revised manuscript.

References

Fierz-Schmidhauser R., Zieger P., Wehrle G., Jefferson A., Ogren J., Baltensperger U., and Weingartner E., Measurement of relative humidity dependent light scattering of aerosols, Atmos. Meas. Tech., 3(1), 39–50, doi:10.5194/amt-3-39-2010, 2010.

Zieger P., Fierz-Schmidhauser R., Weingartner E., and Baltensperger U., Effects of relative humidity on aerosol light scattering: results from different European sites, Atmos. Chem. Phys., 13(21), 10609–10631, doi:10.5194/acp-13-10609-2013, 2013.

Zieger P., Kienast-Sjögren E., Starace M., v. Bismarck J., Bukowiecki N., Baltensperger U., Wienhold F., Peter T., Ruhtz T., Collaud Coen M., Vuilleumier L., Maier O., Emili E., Popp C., and Weingartner E., Spatial variation of aerosol optical properties around the high-alpine site Jungfraujoch (3580 m a.s.l.), Atmos. Chem. Phys., 12, 7231–7249, doi: 10.5194/acp-12-7231-2012, 2012.

Zieger P., Weingartner E., Henzing J., Moerman M., de Leeuw G., Mikkilä J., Ehn M., Petäjä T., Clémer K., van Roozendael M., Yilmaz S., Frieß U., Irie H., Wagner T., Shaiganfar R., Beirle S., Apituley A., Wilson K., and Baltensperger U., Comparison of ambient aerosol extinction coefficients obtained from in-situ, MAX-DOAS and LIDAR measurements at Cabauw, Atmos. Chem. Phys., 11(6), 2603–2624, doi:10.5194/acp-11-2603-2011, 2011.

Zieger P., Fierz-Schmidhauser R., Gysel M., Ström J., Henne S., Yttri K., Baltensperger U., and Weingartner E., Effects of relative humidity on aerosol light scattering in the Arctic, Atmos. Chem. Phys., 10(8), 3875–3890, doi:10.5194/acp-10-3875-2010, 2010.

Revised manuscript with the changes highlighted:

Aerosol light-scattering enhancement due to water uptake during TCAP campaign

G. Titos[1,2], A. Jefferson[3,4], P. J. Sheridan[3], E. Andrews[3,4], H. Lyamani[1,2], L. Alados-Arboledas[1,2], and J. A. Ogren[3]

[1] {Instituto Interuniversitario de Investigación del Sistema Tierra en Andalucía, IISTA-CEAMA, Universidad de Granada, Junta de Andalucía, Granada, 18006, Spain}

[2] {Department of Applied Physic, University of Granada, Granada, 18071, Spain}

[3] {Earth System Research Laboratory, National Oceanic and Atmospheric Administration, Boulder, CO, 80305, United States}

[4] {Cooperative Institute for Research in Environmental Sciences, University of Colorado, Boulder, CO, 80305, United States}

Correspondence to: G. Titos (gtitos@ugr.es)

Abstract

Aerosol optical properties were measured by the DOE/ARM (US Department of Energy Atmospheric Radiation Measurements) Program Mobile Facility during the Two-Column Aerosol Project (TCAP) campaign deployed at Cape Cod, Massachusetts, for a one year period (from summer 2012 to summer 2013). Measured optical properties included aerosol light-absorption coefficient (σ_{ap}) at low relative humidity (RH) and aerosol light-scattering coefficient (σ_{sp}) at low and at RH values varying from 30 to 85%, approximately. Calculated variables included the single scattering albedo (SSA), the scattering Ångström exponent (SAE) and the scattering enhancement factor (f(RH)). Over the period of measurement, f(RH=80%) had a mean value of 1.9±0.3 and 1.8±0.4 in the PM_{10} and PM_1 fractions, respectively. Higher f(RH=80%) values were observed for wind directions from

0-180º (marine sector) together with high SSA and low SAE values. The wind sector from 225 to 315º was identified as an anthropogenically-influenced sector, and it was characterized by smaller, darker and less hygroscopic aerosols. For the marine sector, f(RH=80%) was 2.2 compared with a value of 1.8 obtained for the anthropogenically-influenced sector. The air-mass backward trajectory analysis agreed well with the wind sector analysis. It shows low cluster to cluster variability except for air-masses coming from the Atlantic Ocean that showed higher hygroscopicity. Knowledge of the effect of RH on aerosol optical properties is of great importance for climate forcing calculations and for comparison of in-situ measurements with satellite and remote sensing retrievals. In this sense, predictive capability of f(RH) for use in climate models would be enhanced if other aerosol parameters could be used as proxies to estimate hygroscopic growth. Toward this goal, we propose an exponential equation that successfully estimates aerosol hygroscopicity as a function of SSA at Cape Cod. Further work is needed to determine if the equation obtained is valid in other environments.

1 Introduction

The Earth's atmosphere plays an important role in the planetary energy budget through different processes that shape the Earth's climate. Changes in its composition, even in the less abundant components, like aerosols, can drive climate changes. Aerosol particles actively scatter and absorb radiation as well as change the microphysical properties of clouds. An important factor that can modify the role of aerosols in the global energy budget is the relative humidity (RH). Aerosol particles can take up water, become larger in size than their dry equivalents, and hence, scatter more light. Wet particles may also have different refractive indices and angular scattering properties than their dry counterparts. Continuous measurements of aerosol properties are typically performed under dry conditions (RH<40%) as recommended by international networks such as ACTRIS or GAW (WMO/GAW, 2003). These measurements at low RH can differ from what would be observed at ambient conditions and thus difficult to relate to observations of the radiative energy budget. Therefore, knowledge of the scattering enhancement due to water uptake is of great importance in order to transform dry measurements into more relevant ambient

measurements, especially when comparing in-situ with remote sensing measurements (e.g., Zieger et al., 2011; Zieger et al., 2012; Estéve et al., 2012; Shinozuka et al., 2013) or for satellite retrievals (e.g., Wang and Martin, 2007).

The effect of RH on the aerosol light-scattering coefficient can be determined by means of a tandem nephelometer system (Covert et al., 1972; Fierz-Schmidhauser et al., 2010a, and references therein). Typically, one nephelometer measures at a reference RH (<40%) while the other nephelometer measures at a higher RH. The combination of both measurements allows the determination of the scattering enhancement factor, f(RH), defined as the ratio between the scattering coefficient at high RH and the scattering coefficient at dry conditions. When these measurements are performed by scanning the higher RH over a range of values instead of at constant RH, the evaluation of f(RH) as a function of RH is possible. Different equations have been used to fit f(RH) versus RH. The most widely used equation is a two-parameter, power law fit (e.g., Hänel and Zankl, 1979; Clarke et al., 2002). This equation uses a fit parameter γ to describe the humidity dependence of f(RH) for the entire RH range. The use of γ allows the comparison of measurements taken at different RH values. Carrico et al. (2003) describes several other fitting techniques as well, applied to different RH ranges.

Many studies have been published assessing the impact of RH on the aerosol light scattering coefficient for different aerosol types such as urban (Yan et al., 2009), free troposphere (Fierz-Schmidhauser et al., 2010b), continental (e.g., Sheridan et al., 2001; Pan et al., 2009) and marine aerosols (e.g., McInnes et al., 1998; Fierz-Schmidhauser et al., 2010c). Much of the recent research was performed in Central European sites (Zieger et al., 2013) and was focused on short measurement campaigns of one to four months duration. While there are a fair number of f(RH) ground based studies on a variety of aerosol types, very few of them have provided information on the aerosol scattering enhancement of fine mode aerosols; although some exceptions can be found in the literature (e. g., McInnes et al., 1998; Koloutsou-Vakakis et al., 2001; Sheridan et al., 2001; Carrico et al., 2003; Fierz-Schmidhauser et al., 2010a).

In this work, aerosol optical properties in two size ranges (D_p < 1 μm and D_p < 10 μm) were measured over a one year period at Cape Cod (Massachusetts, USA) during the Two-

Column Aerosol Project (TCAP) campaign. Information concerning aerosol hygroscopicity is available for 7 months of the campaign. The main goals of this work are to characterize the hygroscopic scattering enhancement during the TCAP campaign and to explore the different situations and factors that led to changes in the hygroscopicity, as well as to explore the use of dry optical properties as proxies to estimate the hygroscopic enhancement.

2 Experimental site and instrumentation

2.1 Site description

The measurements presented in this study were conducted by the DOE/ARM (US Department of Energy Atmospheric Radiation Measurements) Program Mobile Facility (Miller and Slingo, 2007; Mather and Voyles, 2013) during the Two-Column Aerosol Project (TCAP) campaign (Kassianov et al., 2013) deployed at Cape Cod, Massachusetts. Cape Cod is a peninsula jutting out into the Atlantic Ocean in the easternmost portion of the state of Massachusetts, in the northeastern United States. The deployment was located in the northeastern part of the cape (41°59'36'' N, 70°03'01'' W, 20 m a.s.l.), inside the Cape Cod National Seashore, and relatively close to large urban agglomerations such as Providence and Boston. Thus, due to its location, the site is subject to both clean and polluted conditions. The campaign started in the summer of 2012 and lasted until the summer of 2013; however, due to problems with the humidifier system, measurements of the hygroscopic enhancement are only available for approximately half of the campaign (from late September to late October 2012 and then from January to mid June 2013).

2.2 Instrumentation

Air sampling for all the instrumentation used in this study was obtained from the top of a 10 m high sampling stack of 20.3 cm in diameter. Airflow through this main stack is about 800 lpm. From this flow, 150 lpm flow through a 5.1 cm diameter stainless steel pipe in the center of this larger flow that then is divided into five 30-lpm sample lines. One of these sample lines goes to the Aerosol Observing System (AOS) instruments and the other 4 spare sample lines go out through a blower. A more detailed description of the sampling system can be found in Jefferson (2011).

The experimental set-up consists of two integrating nephelometers (TSI, model 3563) operated in series and separated by a humidifier system. Since no active drying of the aerosol sample is performed after humidification only the lower branch of the hysteresis curve can be captured with this set-up. The integrating nephelometer (TSI, model 3563) measures aerosol light-scattering (σ_{sp}) and hemispheric backscattering (σ_{bsp}) coefficients at three wavelengths (450, 550 and 700 nm). Instrument zero checks on filtered air were automatically performed hourly. Routine maintenance and instrument calibrations with CO_2 were performed 3 times; once in July, another in January and again in June. The nephelometers are downstream of a switched impactor system which toggles the aerosol size cut between 1.0 µm (PM_1) and 10 µm (PM_{10}) aerodynamic particle diameters every 30 minutes. The first nephelometer measures the aerosol light-scattering coefficient at dry conditions (RH<40%) while the second nephelometer measures the aerosol light-scattering coefficient at a controlled RH. The sampled aerosol was gently heated when necessary to achieve a low relative humidity (RH) of 40% or below. The mean ± standard deviation of the temperature and relative humidity within the dry nephelometer for the whole measurement campaign were T = 26±4 ºC and RH = 30±13 %. In order to minimize losses of volatile compounds the temperature of the sampled air was kept below 35 ºC (Bergin et al., 1997; ten Brink et al., 2000). Only 0.5% of the 1-min observations occurred at temperatures above this value and these data were not further considered in the study. The humidifier consists of two concentric tubes: the inner one is a high-density porous polytetrafluoroethylene (PTFE) tube and the outer tube is a stainless steel tube wrapped in a tape heater and insulation. A closed loop of water circulates between the PTFE and the outer tube. As the water temperature increases, water vapor moves through the semi-permeable PTFE membrane causing the RH of the sample air to increase. The temperature of the water is regulated via a feedback system between the downstream RH sensor, the PID (proportional-integral-derivative) controller and the heater. Temperature and relative humidity sensors (Vaisala model HMP110, accuracy of ±3% RH) are placed throughout the system: one of the sensors is placed upstream of the impactor box and the other two sensors are placed immediately downstream of the reference and humidified nephelometers. The internal nephelometer TSI RH sensors are not used because of their slower time response and uncertainty. For this reason, the RH inside the nephelometer was calculated from the

dew point temperature of the Vaisala sensor at the outlet of the humidified nephelometer and the internal nephelometer temperature. The instruments reported results at 1-Hz resolution, and the data were then averaged and recorded at 1 min resolution. The nephelometers operated at a volumetric flow rate of 30 lpm. Non-idealities due to truncation errors and the non-Lambertian light source were corrected according to Anderson and Ogren (1998). The uncertainty in the aerosol light-scattering coefficient is about 7% (Heintzenberg et al., 2006). Every hour the RH measurement cycle started with a zero measurement and then in the humidified nephelometer the RH was increased stepwise to 80-85% within 30 min, and then decreased back to RH values of about 40% or below during the second half of the hour. The upward RH scan corresponded to the PM_{10} size cut and the downward RH scan to PM_1. When both nephelometers measured at dry conditions (RH<40%) the two of them agreed well (PM_{10}: slope = 1.073±0.001, intercept = 0.48±0.02 Mm^{-1} and R^2 = 0.99; PM_1: slope = 0.971±0.004, intercept = 0.68±0.04 Mm^{-1} and R^2 = 0.77 (for the 550 nm wavelength)).

The aerosol light absorption coefficient was measured with a Particle Soot Absorption Photometer (PSAP). The method is based on the integrating plate technique in which the change in optical transmission of a filter caused by particle deposition on the filter is related to the light absorption coefficient of the deposited particles using Beer-Lambert Law. Here, a 3-wavelength version of the PSAP has been used, with nominal wavelengths of 467 nm, 531 nm, and 650 nm. The PSAP data were corrected according to Bond et al. (1999) and Ogren (2010). The uncertainty of the PSAP absorption measurement, after application of the transmission and scattering correction, is 20–30% (Bond et al., 1999). The PSAP is also downstream of the switched impactors.

Ambient temperature, relative humidity, wind speed and direction were continuously monitored using the surface meteorological instrumentation (MET) data from the ARM AMF1 facility.

Air mass back trajectories were computed using the HYSPLIT4 model (Draxler et al., 2009) version 4.9 and were used to support the interpretation of the data.

3 Methodology

Aerosol intensive properties, such as the single scattering albedo (SSA), the hemispheric backscatter fraction (b), the submicron scattering fraction (R_{sp}) and scattering Ångström exponent (SAE), were calculated from the aerosol scattering and/or absorption coefficients.

The scattering Ångström exponent characterizes the wavelength dependence of σ_{sp} and was calculated using the 700 nm and 450 nm wavelength pair using the following equation:

$$SAE(\lambda_1 - \lambda_2) = -(\log\sigma_{sp}(\lambda_1) - \log\sigma_{sp}(\lambda_2))/(\log\lambda_1 - \log\lambda_2) \quad (1)$$

This variable increases with decreasing particle size and typically has values around 2 or higher when the scattering process is dominated by fine particles, while it is close to 0 when the scattering process is dominated by coarse particles (Delene and Ogren, 2002).

The submicron scattering fraction allows apportionment of light scattering into sub- and super-micrometer aerosol mode. It was calculated for the 550 nm wavelength as follows:

$$R_{sp}(\lambda) = \sigma_{sp(Dp < 1\ \mu m)}(\lambda)/\ \sigma_{sp(Dp < 10\ \mu m)}(\lambda) \quad (2)$$

The hemispheric backscatter fraction is the fraction of radiation that is scattered back at angles between 90-170°. This parameter increases with decreasing particle size.

$$b(\lambda) = \sigma_{bsp}(\lambda) / \sigma_{sp}(\lambda) \quad (3)$$

The aerosol single scattering albedo at 550 nm wavelength is the ratio of the scattering and extinction coefficients. It was calculated using the following formula:

$$SSA(\lambda) = \sigma_{sp}(\lambda) / (\sigma_{sp}(\lambda) + \sigma_{ap}(\lambda)) \quad (4)$$

In order to determine SSA at 550 nm, the absorption coefficient measured with the PSAP was interpolated to the 550 nm wavelength using the above described Ångström formula. In this work, SSA(550), b(550), R_{sp}(550) and SAE(450-700) refer always to dry conditions and to the PM_{10} size fraction.

To quantify the effect of water uptake in the aerosol light scattering coefficient, the scattering enhancement factor f(RH) defined as the ratio of $\sigma_{sp}(\lambda)$ at a high and at reference RH (λ = 550 nm in the present work) was used and calculated as follows:

$$f(RH, \lambda) = \sigma_{sp}(RH, \lambda) / \sigma_{sp}(dry, \lambda) \quad (5)$$

This study uses the following two-parameter equation (Clarke et al., 2002; Carrico et al., 2003) to describe the increase in aerosol scattering due to hygroscopic growth:

$$f(RH) = a\,(1\text{-}RH)^{-\gamma} \quad (6)$$

where a is the intercept at RH = 0% and γ parameterizes the magnitude of the scattering enhancement. To reduce the influence of instrument noise on the calculation, only values of the dry scattering coefficient above 5 Mm^{-1} were considered in the calculation of f(RH). The constraints imposed for the fitting were a lower RH of 40%, a minimum span of 30% RH in each scan, a minimum of 50% data coverage in each scan, the RH in the reference nephelometer had to be below 40% and a fit R^2 value above 0.5. These criteria were applied for PM_{10} and PM_1 size fractions, with each size fraction fitted separately. A total of 2952 (PM_{10}) and 1753 (PM_1) humidograms were successfully fitted for each size respectively. Additionally, for each scan, f(RH) values were calculated at RH=80% using equation 6, enabling comparison of scan hygroscopicity.

4 Results and discussion

4.1 Overview of the campaign

Mean ambient temperature and relative humidity during the campaign were 7±6 °C and 80±20 %. Both variables presented clear diurnal patterns with higher temperature and lower RH values at midday. The wind speed ranged from calm winds up to values close to 20 m/s during specific periods, showing a mean campaign value of 5±3 m/s. Winds from the west direction occurred more frequently. Figure 1 shows an overview of the daily average aerosol light-scattering and absorption coefficients, $\sigma_{sp}(550)$ and $\sigma_{ap}(531)$, single scattering albedo, SSA(550), and scattering Ångström exponent, SAE(450-700), in the PM_{10} fraction. For the entire campaign, the $\sigma_{sp}(550)$ had a mean ± standard deviation value of 22±15 Mm^{-1} and the corresponding values for $\sigma_{ap}(531)$ were 1.1±0.9 Mm^{-1}. In general, the aerosol light absorption coefficient was very low during the measurement period, especially compared with the scattering coefficient; the SSA(550) had a mean value of 0.94±0.04. On the other hand, daily-average SSA(550) values ranged from 0.77 to 1.0, denoting periods where the contribution of absorption increased. The campaign-averaged SAE(450-700) was 1.8±0.6, which is quite high for a coastal environment compared with literature values (e.g., Carrico

et al., 1998; Fierz-Schmidhauser et al., 2010b), and is an evidence of the influence of anthropogenic aerosols at Cape Cod during TCAP campaign. In fact, the SAE(450-700) showed a high variability with daily values ranging from 0.6 to 3. The submicron scattering fraction reported similar information with values ranging from 0.02 to 1 indicating different atmospheric conditions dominated by different aerosol types (fine, coarse and mixed particles). Concerning the backscatter fraction, this variable had a mean campaign value of 0.13±0.02. The SAE(450-700), $R_{sp}(550)$ and b(550) report similar information since all three parameters are related to aerosol mean size (Fan et al., 2014). In fact, the SAE(450-700) had a strong correlation with R_{sp} (R^2 = 0.81) and a moderate correlation with b (R^2 = 0.5), both at 550 nm. For this reason, in the following sections we will focus on the scattering Ångström exponent as indicator of particle size.

None of the variables mentioned above showed a clear diurnal pattern, presenting very small changes throughout the day. In addition, no clear temporal trend was observed throughout the study period, although certain events of elevated $\sigma_{sp}(550)$ were observed connected with high SSA(550) values and low SAE(450-700) values. These events occurred under high wind speeds and were probably caused by sea salt particles (large particles with minimal absorption). As an example, on 9 March the $\sigma_{sp}(550)$ reached its maximum value (daily average of 84 Mm^{-1}). On this day the SSA had a mean value of 1 and the SAE was 0.75, suggesting that the aerosol optical properties were dominated by coarse, purely scattering particles.

Figure 2 shows the aerosol light scattering enhancement factor f(RH=80%) (upper panel) and the γ parameter (lower panel) calculated for the PM_{10} and PM_1 fractions at 550 nm (hereafter the wavelength will be omitted in the notation for simplicity). Over the period of measurement, f(RH=80%) had a mean value of 1.9±0.3, with daily-mean values ranging from 1.4 to 2.6 in the PM_{10} fraction. In the PM_1 fraction, f(RH=80%) had a mean value of 1.8±0.4 and ranged from 1.2 to 3.4. Average γ values were 0.5 for both size fractions but were relatively more variable in the PM_1 fraction (in PM_1, daily γ values ranged from 0.1 to 1.1, and in PM_{10} ranged from 0.2 and 0.9). The temporal trend of f(RH=80%) and γ was similar in both size fractions, however, larger differences between PM_{10} and PM_1 were observed for specific events. Specifically, on 9 March this difference was considerably larger with a mean daily f(RH=80%) of 3.1 in PM_1 compared to 2.4 in PM_{10}. On this day,

the air mass back-trajectories arriving at 500 m a.g.l. at the measurement station were coming from the Atlantic Ocean and traveled at low altitude for the last three days, likely picking up sea salt particles. In order to investigate in more detail the differences in the magnitude of the scattering enhancement between the fine and coarse fractions, Figure 3 shows the hourly f(RH=80%) values in PM_1 versus f(RH=80%) values in PM_{10}. Data when the SAE (at dry conditions and in the PM_{10} fraction) was below and above 1, denoting a predominance of larger and smaller particles, respectively, were fitted separately. The graph shows that for situation dominated by aerosol sea salt (SAE<1) the scattering in the PM_1 fraction experienced a higher enhancement than in the PM_{10} fraction. This same behavior was also found for the γ parameter (not shown). This indicates that small sea salt particles have a larger scattering enhancement compared to coarse sea salt particles. This result is supported by theoretical calculations of hygroscopic growth as a function of particles size for common aerosol salts and acids made by Zieger et al. (2013). These authors showed that f(RH=85%) increases with decreasing particle size for all components studied, but increases more dramatically for NaCl, the largest component in sea salt. On the other hand, this behavior can be also explained by a shift in the size distribution to a scattering regime with a higher scattering efficiency when the SAE is greater than 1.

A total of 2952 and 1753 RH scans in PM_{10} and PM_1 fractions, respectively, were fitted according to the criteria explained in Section 3. Additional fits were performed for the RH ranges below and above 65%. The values of $\gamma_{>65\%}$ and $\gamma_{<65\%}$ were used to identify possible deliquescence transitions. Similar values of $\gamma_{>65\%}$ and $\gamma_{<65\%}$ indicate a monotonic growth for the entire RH range, while distinct values ($\gamma_{<65\%} << \gamma_{>65\%}$) indicate no significant enhancement below 65% and a large increase at an RH value above 65%. For those cases in which $\gamma_{<65\%} << \gamma_{>65\%}$ the fit using the entire RH range underestimated f(RH) values at both low and high RH and overestimated f(RH) at the transition RH (around 65-75% RH). To illustrate this, Figure 4a and Figure 4b show the daily average humidograms for two different cases dominated by deliquescent and non-deliquescent particles, respectively. Figure 4a shows 9 March daily average humidogram scan (γ = 0.8, $\gamma_{<65\%}$ = 0.4 and $\gamma_{>65\%}$ = 1.1) and Figure 4b shows the daily average humidogram scan of 31 May (γ = 0.3, $\gamma_{<65\%}$ =0.3 and $\gamma_{>65\%}$ = 0.4). On 9 March the scattering enhancement for RH>65% was almost three fold the enhancement for RH<65%. As mentioned before, during this day there was a

predominance of non-absorbing coarse particles (mean SAE(450-700) = 0.75 and SSA(550) = 1), suggesting a clear contribution of deliquescent sea salt particles. On the other hand, on 31 May the scattering enhancement was similar for both RH ranges. Slightly darker, non-deliquescent fine mode particles dominated the aerosol on 31 May (SAE(450-700) = 1.8, SSA(550) = 0.91) compared with the previous case. Concerning the "a" parameter, it varies with the aerosol transmission efficiency through the humidifier and goodness of the power law fit. Differences between the experimental and ideal value of "a" are expected since the "a" value will depend also on aerosol losses in the dry nephelometer and in the humidifier system. In this study, fitting the whole RH range for deliquescent aerosols seems to be inadequate. Nevertheless, fitting f(RH) to multiple RH ranges offers information on aerosol deliquescence properties.

4.2 Influence of wind speed and direction on the aerosol hygroscopicity

In order to evaluate the influence of wind speed and direction on aerosol hygroscopic properties, Figure 5 shows bivariate plots of f(RH=80%), γ, SSA(550) and SAE(450-700) as a function of wind speed and direction (Openair software, Carslaw and Ropkins, 2012). Both f(RH=80%) and γ increased with wind speed. SSA(550) and SAE(450-700) have opposite trends to each other, with increasing SSA(550) values and decreasing SAE(450-700) with wind speed These plots show that there is a region between approximately 225 and 315º, characterized by lower SSA(550) and higher SAE(450-700), probably influenced by anthropogenic air from the populated urban areas of Providence and Boston. In contrast, the region from 0 to 180º, characterized by higher SSA(550) and lower SAE(450-700), can be considered as marine dominated aerosols from the North Atlantic ocean. According to these results, two wind sectors have been considered for further investigation: the marine sector (0-180º) and the anthropogenically-influenced sector (225-315º). For this analysis, only wind speed values above 5 m/s were considered in order to avoid local influences. The marine wind sector was characterized by slightly higher temperatures and RH values (median values: T = 4.9 and RH = 89%) than the anthropogenically-influenced wind sector (T = 2.4 °C and RH = 58%). This last sector also showed a higher variability in the temperature values. Table 1 summarizes the mean and standard deviation of the aerosol optical parameters for each sector. There is a clear difference between both wind sectors

when looking at the aerosol intensive properties. The anthropogenically-influenced sector was characterized by smaller and more absorbing particles with similar f(RH=80%) for both size fractions. Furthermore, for the anthropogenically-influenced sector, $\gamma_{>65\%}$ and $\gamma_{<65\%}$ were very similar denoting no distinct deliquescent behavior. The marine sector presented very different properties compared with the anthropogenic sector: it was characterized by larger and very weakly absorbing particles (see Table 1). The f(RH=80%) was higher in the PM_1 than PM_{10} fraction, denoting a larger scattering enhancement in the fine mode. In addition, $\gamma_{>65\%}$ was considerably higher (0.9±0.2) than $\gamma_{<65\%}$ (0.4±0.1), evidence of deliquescent aerosols. Carrico et al. (2000) also observed a higher scattering enhancement for clean marine conditions than for polluted situations (see Table 2) in Sagres (Portugal) which agrees with the results obtained in this section (Table 1) and those shown in Figure 3. The f(RH) values reported here for clean and anthropogenically influenced marine aerosols are in agreement with the range of values reported in the literature (Table 2).

4.3 Air-mass trajectories classification

A cluster analysis of 3-day air mass backtrajectories arriving at Cape Cod at 500 m a.g.l. at 00, 06, 12 and 18 GMT using HYSPLIT4 model (Draxler et al., 2009) version 4.9 was performed to identify the main air masses types affecting the area and their respective aerosol optical properties. This method is based on the geometric distance between individual trajectories and it takes into account speed and direction of the trajectory and height at the arriving location. A total of 1344 backward trajectories were used in the analysis. The number of clusters was selected according to the percent change in total spatial variance (TSV). Large changes in the TSV were interpreted as the merging of significantly different trajectories into the same cluster. According to this criterion, the cluster analysis resulted in five clusters of backtrajectories for air masses arriving at Cape Cod at low level. Figure 6 shows the clusters obtained with this analysis and the average humidogram for each cluster. The humidograms represent f(RH) averages in 2% RH size bins and the error bars represent the standard deviation in the PM_{10} fraction. Table 3 shows, for each cluster, the mean and standard deviation of the optical parameters. Clusters 1-4 exhibited similar aerosol optical properties with only small differences. Cluster 5 was characterized by small SAE(450-700) and high SSA(550), as well as by high γ and

f(RH=80%) values. The air masses included in this cluster came from the north-east, some of them originating as far away as Greenland, passing over sparsely-populated regions and the Atlantic Ocean. The high SAE(450-700) for cluster 4 together with a lower SSA(550) denotes an anthropogenic influence. Clusters 3 and 4 had similar characteristics in terms of the aerosol optical properties (see Figure 6 and Table 3). Both clusters comprise continental air masses. Clusters 1 and 2 had hybrid properties: with a predominance of larger particles compared to cluster 3 and 4 and with higher SSA values. This is probably because the air masses in clusters 1 and 2 passed over open Ocean but originated in polluted continental regions. The cluster to cluster variation in the aerosol optical properties can be explained by the degree of anthropogenic and marine influence in the air masses included in each cluster.

4.4 Relationship between γ and SSA and SAE

Predictive capability and global coverage of aerosol hygroscopicity for use in climate models would be enhanced if other aerosol parameters could be used as proxies to estimate hygroscopic growth. Toward this goal, we examined covariances between γ and aerosol intensive properties. Figure 7 shows the frequency distribution of γ in the PM_{10} fraction for different SAE and SSA ranges. Values of SAE(450-700) below 1 denote a higher predominance of coarse particles and lower SSA(550) values indicate darker aerosols. From Figure 7b, it is clear that aerosols containing a higher fraction of absorbing particles (lower SSA) are less hygroscopic since the frequency distribution is shifted towards lower γ values. In contrast, Figure 7a suggest that when coarse aerosols predominate (SAE<1) the hygroscopic enhancement is larger. In general, γ decreased as the contribution of coarse particles decreased, that is, as SAE increased (the correlation coefficient of γ versus SAE was R = -0.77). This result contrasts with the result of Zieger et al. (2010) that showed a decrease of γ for an increase in the contribution of coarse particles (R = 0.34), probably connected with compensating effects of different varying aerosol properties during their study.

Because the γ frequency distribution segregates well between high and low values of SSA and SAE, these variables seem to be good candidates as proxies to estimate the scattering enhancement due to water uptake. Based on the previous results, the following question arises: Can the aerosol hygroscopicity be predicted based on dry optical properties? To

answer this question, Figure 8 (upper panel) shows γ versus SSA(550) where the color code represents the range of SAE(450-700). Figure 8a refers to γ in PM_1 and Figure 8b refers to γ in PM_{10}. In both γ graphs, SAE(450-700) and SSA(550) corresponds to the PM_{10} size fraction and to dry conditions. The PM_1 γ was referenced to PM_{10} SSA and SAE as a means to make the fits applicable to surface measurements which may have only PM_{10} data and still differentiate the total and fine mode aerosol for models. As SSA(550) values increase the contribution of coarse particles also increases and these particles become more hygroscopic (bluish colors in Figure 8). The increase of γ with SSA in 550 nm wavelength is well described by the following exponential functions for the PM_1 (equation 7) and PM_{10} (equation 8) size fractions respectively:

$$\gamma = (3\pm5)\cdot10^{-15} e^{\frac{SSA}{(0.030\pm0.001)}} + (0.31\pm0.01) \qquad (7)$$

$$\gamma = (4\pm3)\cdot10^{-9} e^{\frac{SSA}{(0.054\pm0.002)}} + (0.26\pm0.01) \qquad (8)$$

The coefficient of determination was $R^2 = 0.76$ in PM_1 and $R^2 = 0.77$ in PM_{10}. The increase observed in γ for higher SSA(550) values is more pronounced in the PM_1 than in the PM_{10} size fractions. Figure 8 (lower panel) shows the frequency distribution of the residuals for the fit in PM_1 and in PM_{10}, respectively, in order to assess the quality of the regression. About 79% of the γ values in PM_1 and 92% in PM_{10} were estimated by the model with a difference of ±0.15 in γ. The residuals did not exhibit any dependence on SAE, suggesting that the exponential fit captures most of the covariance between SAE and SSA. The potential of this model lies in its simplicity, as the aerosol hygroscopicity can be estimated by a single parameter, the dry single scattering albedo. Quinn et al. (2005) proposed a parameterization based on the aerosol chemical composition, in particular, in the fraction of particulate organic matter to predict f(RH). Also based on the chemical composition, Garland et al. (2007) reported that the f(RH=80%) varied linearly with the organic/inorganic content. However, measurements of aerosol chemical composition are commonly performed once a week and integrated over a 24 hour period whereas optical properties are continuously measured at high time resolution. In this particular study, the coarse mode was predominantly dominated by sea salt particles and the presence of other species that typically accumulate in the coarse fraction like dust particles was negligible. Due to the similar characteristics of sea salt and dust particles in terms of SAE and SSA,

but the strong difference in the hygroscopic behavior, the parameterization proposed in this study would fail under the presence of both types of aerosols as pure dust aerosols does not experience significant hygroscopic growth. The Cape Cod study may be considered as representative of an aerosol from the Northern Atlantic coast with anthropogenic influence. The same analysis needs to be applied to other regions and aerosol types to catalog exponential fit parameters of γ versus SSA over a variety of aerosol types and atmospheric conditions.

5 Conclusions

The measured f(RH) dependency with RH during TCAP campaign can be well described with an empirical two-parameter fit equation for both size fractions (PM_1 and PM_{10}). During the study period, f(RH=80%) and the fit parameter γ in PM_{10} had a mean value of 1.9 and 0.5, respectively. Two distinct sectors were identified according to wind speed and direction. For the marine sector (wind speed above 5 m/s and wind direction between 0 and 180 degrees), the γ parameter had a mean value of 0.7±0.1 for $\gamma_{>65\%}$, which was considerably higher than for $\gamma_{<65\%}$. The sharp increase in f(RH) at an RH above 65% indicated the aerosol deliquescence. The anthropogenically-influenced sector (wind speed above 5 m/s and wind direction between 225 and 315 degrees) was characterized by a predominance of smaller and darker aerosols with lower hygroscopicity. The enhanced fine mode hygroscopic growth was more pronounced for sea salt aerosol than for mixed or anthropogenic aerosol. The air-mass trajectory classification analysis agreed with the wind sector analysis. Small differences were found between clusters, with the exception of cluster 5 that corresponds to clean marine air masses.

A clear relationship between the intensive parameters SSA and SAE with γ was observed. The γ parameter increased for increasing SSA and decreasing SAE values, that is, larger and less absorbing particles tended to be more hygroscopic. An exponential equation which fit γ to a single parameter (the single scattering albedo) was found to have a relatively low residual error, suggestion that SSA was a good proxy of the aerosol scattering hygroscopic growth. The Cape Cod study represents aerosol from a Northern Atlantic coastal site with influence of marine and anthropogenic aerosols. The same analysis needs to be applied to

other regions and aerosol types to catalog exponential fit parameters of γ versus SSA over a variety of aerosol types and atmospheric conditions. This particular study had a strong covariance between SSA and SAE, which allowed a reduction in the γ fit to a single parameter, SSA. Other sites with smoke, dust or with strong differences in aerosol composition between the fine and coarse mode may require more fit parameters.

Acknowledgments

This research was funded by the NOAA Climate Program using measurements funded by the U.S. Department of Energy Atmospheric System Research program. The authors would like to express their gratitude to the NOAA Air Resources Laboratory (ARL) for the provision of the HYSPLIT transport and dispersion model. We would like to thank also the Openair project. G. Titos was funded by Spanish Ministry of Economy and Competitiveness – Secretariat of Science, Innovation and Development under grants BES-2011-043721 and EEBB-I-13-06456, and projects P10-RNM-6299, CGL2010-18782 and EU INFRA-2010-1.1.16-262254.

References

Anderson, T.L., and Ogren, J. A.: Determining aerosol radiative properties using the TSI 3563 integrating nephelometer, Aerosol Sci. Technol., 29, 57–69, 1998.

Bergin, M. H., Ogren, J. A., Schwartz, S.E. and McInnes, L. M.: Evaporation of ammonium nitrate aerosol in a heated nephelometer: Implications for field measurements. Environ. Sci. Technol., 31, 2878–2883, 1997.Bond, T. C., Anderson, T. L. and Campbell, D.: Calibration and intercomparison of filter-based measurements of visible light absorption by aerosols. Aerosol Sci. Technol., 30, 582– 600, 1999.

Carrico, C.M., Rood, M.J. and Ogren, J.A.: Aerosol light scattering properties at Cape Grim, Tasmania, during the First Aerosol Characterization Experiment (ACE 1), J. Geophys. Res., 103, D13, 16565-16574, 1998.

Carrico, C. M., Rood, M. J., Ogren, J. A., Neusüb, C., Wiedensohler, A. and Heintzenberg, J.: Aerosol optical properties at Sagres, Portugal during ACE-2, Tellus, 52B, 694-715, 2000.

Carrico, C. M., Kus, P., Rood, M. J., Quinn, P. K. and Bates, T. S.: Mixtures of pollution, dust, sea salt, and volcanic aerosol during ACE-Asia: Radiative properties as a function of relative humidity, J. Geophys. Research., 108, D23, 8650, 2003.

Carslaw, D. C. and Ropkins, K.: Openair- An R package for air quality data analysis, Environmental Modelling & Software, 27-28, 52-61, 2012.

Clarke, A. D., Howell, S., Quinn, P. K., Bates, T. S., Ogren J. A., Andrews, E., Jefferson, A., Massling, A., Mayol-Bracero, O., Maring, H., Savoie, D., and Cass, G.: INDOEX aerosol: A comparison and summary of chemical, microphysical, and optical properties observed from land, ship, and aircraft, J. Geophys. Res., 107, 8033, doi:803310.1029/2001JD000572, 2002.

Covert, D. S., Charlson, R. J. and Ahlquist, N. C.: A study of the relationship of chemical composition and humidity to light scattering by aerosols, Journal of Applied Meteorology, 11, 968-976, 1972.

Delene, D. J. and Ogren, J. A.: Variability of Aerosol Optical Properties at Four North American Surface Monitoring Sites, J. Atmos. Sci., 59, 1135–1149, 2002.

Draxler, R.R., Stunder, B., Rolph, G. and Taylor, A.: HYSPLIT4 User's Guide. NOAA Air Resources Laboratory, 2009.

Estéve, A. R., Ogren, J. A., Sheridan, P. J., Andrews, E., Holben, B. N. and Utrillas, M. P.: Sources of discrepancy between aerosol optical depth obtained from AERONET and in-situ aircraft profiles, Atmos. Chem. Phys., 12, 2987-3003, 2012.

Fan, X., Chen, H., Xia, X., Li, Z. and Cribb, M.: Aerosol optical properties from the Atmospheric Radiation Measurement Mobile Facility at Shouxian, China, J. Geophys. Res., 115, D00K33, doi:10.1029/2010JD014650, 2010.

Fierz-Schmidhauser, R., Zieger, P., Wehrle, G., Jefferson, A., Ogren, J.A., Baltensperger, U. and Weingartner, E.: Measurement of relative humidity dependent light scattering of aerosols, Atmos. Meas. Tech., 3, 39-50, 2010a.

Fierz-Schmidhauser, R., Zieger, P., Gysel, M., Kammermann, L., DeCarlo, P. F., Baltensperger, U. and Weingartner, E.: Measured and predicted aerosol light scattering enhancement factors at the high alpine site Jungfraujoch, Atmos. Chem. Phys., 10, 2319-2333, 2010b.

Fierz-Schmidhauser, R., Zieger, P., Vaishya, A., Monahan, C., Bialek, J., O'Dowd, C. D., Jennings, S. G., Baltensperger, U. and Weingartner, E.: Light scattering enhancement factors in the marine boundary layer (Mace Head, Ireland), J. Geophys. Res., 115, D20204, 2010c.

Garland, R. M., Ravishankara, A. R., Lovejoy, E. R., Tolbert, M. A. and Baynard, T.: Parameterization for the relative humidity dependence of light extinction: Organic-ammonium sulfate aerosol, J. Geophys. Res., 112, D19303, 2007.

Gassó, S., Hegg, D. A., Covert, D. S., Collins, D., Noone, K. J., Öström, E., Schmid, B., Russell, P. B., Livingston, J. M., Durkee, P. A. and Jonsson, H.: Influence of humidity on the aerosol scattering coefficient and its effect on the upwelling radiance during ACE-2, Tellus, 52B, 546-567, 2000.

Hänel, G. and Zankl, B.: Aerosol size and relative humidity: Water uptake by mixtures of salts, Tellus, 31, 478-486, 1979.

Hegg, D. A., Covert, D. S., Rood, M. J. and Hobbs, P. V.: Measurements of aerosol optical properties in marine air, J. Geophys. Res., 101, D8, 12893-12903, 1996.

Heintzenberg, J., Wiedensohler, A., Tuch, T. M., Covert, D. S., Sheridan, P., Ogren, J. A., Gras, J., Nessler, R., Kleefeld, C., Kalivitis, N., Aaltonen, V., Wilhelm, R. T., and Havlicek, M.: Intercomparisons and aerosol calibrations of 12 commercial integrating nephelometers of three manufacturers, J. Atmos. Ocean. Tech., 23, 902–914, 2006.

Jefferson, A.: Aerosol Observing System (AOS) Handbook, U. S. Department of Energy, DOE/SC- ARM/TR-014, (Available at http://www.arm.gov/publications/tech_reports/handbooks/aos_handbook.pdf), 2011.

Kassianov, E., Barnard, J., Pekour, M., Berg, L. K., Fast, J., Michalsky, J., Lantz, K. and Hodges, G.: Temporal variability of aerosol properties during TCAP: Impact on radiative forcing, Proc. SPIE8890, doi:10.1117/12.2029355, 2013.

Koloutsou-Vakakis, S., Carrico, C. M., Kus, P., Rood, M. J., Li, Z., Shrestha, R., Ogren, J. A., Chow, J. C. and Watson, G.: Aerosol properties at a midlatitude Northern Hemisphere continental site, J. Geophys. Res., 106, D3, 3019-3032, 2001.

Kotchenruther, R. A., Hobbs, P. V. and Hegg, D. A.: Humidification factors for atmospheric aerosols off the mid-Atlantic coast of the United States, J. Geophys. Res., 104, D2, 2239-2251, 1999.

Li-Jones, X., Maring, H. B. and Propero, J. M.: Effect of relative humidity on light scattering by mineral dust aerosol as measured in the marine boundary layer over the tropical Atlantic Ocean. J. Geophys. Res., 103, D23, 31113-31121, 1998.

Mather, J. H. and Voyles, J. W.: The Arm Climate Research Facility: A Review of Structure and Capabilities. Bull. Amer. Meteor. Soc., 94, 377–392, doi: http://dx.doi.org/10.1175/BAMS-D-11-00218.1, 2013.

Miller, M. A. and Slingo, A.: The ARM Mobile Facility and its first international deployment: Measuring Radiative Flux Divergence in West Africa. Bull. Amer. Meteor. Soc., 88, 1299-1244, doi:10.1175/BAMS-88-8-1229, 2007.

McInnes, L., Bergin, M., Ogren, J. A. and Schwartz, S.: Apportionment of light scattering and hygroscopic growth to aerosol composition, Geophys. Res. Lett., 25, 4, 513-516, 1998.

Ogren, J. A.: Comment on "Calibration and Intercomparison of Filter-Based Measurements of Visible Light Absorption by Aerosols", Aerosol Sci. Tech., 44:589-591, 2010.

Pan, X. L., Yan, P., Tang, J., Ma, J. Z., Wang, Z. F., Gbaguidi, A. and Sun, Y. L.: Observational study of influence of aerosol hygroscopic growth on scattering coefficient over rural area near Beijing mega-city, Atmos. Chem. Phys., 9, 7519-7530, 2009.

Quinn, P. K., Bates, T. S., Baynard, T., Clarke, A. D., Onasch, T. B., Wang, W., Rood, M. J., Andrews, E., Allan, J., Carrico, C. M., Coffman, D. and Wornsnop, D.: Impact of particulate organic matter on the relative humidity dependence of light scattering: A simplified parameterization, Geophys. Res. Lett., 32, L22809, 2005.

Sheridan, P.J., Delene, D. J. and Ogren, J. A.: Four years of continuous surface aerosol measurements from the Department of Energy's Atmospheric Radiation Measurement Program Southern Great Plains Cloud and Radiation Testbed site, J. Geophys. Res., 106, D18, 20735-20747, 2001.

Sheridan, P. J., Jefferson, A. and Ogren, J. A.: Spatial variability of submicrometer aerosol radiative properties over the Indian Ocean during INDOEX, J. Geophys. Res., 107, D19, 8011, 2002.

Shinozuka, Y., Johnson, R. R., Flynn, C. J., Russell, P. B., Schmid, B., Redemann, J., Dunagan, S. E., Kluzek, C. D., Hubbe, J. M., Segal-Rosenheimer, M., Livingston, J. M., Eck, T. F., Wagener, R., Gregory, L., Chand, D., Berg, L. K., Rogers, R. R., Ferrare, R. A., Hair, J. W., Hostetler, C. A. and Burton, S. P.: Hyperspectral aerosol optical depths from TCAP flights, J. Geophys. Res., Accepted, doi: 10.1002/2013JD020596, 2013.

ten Brink, H. M., Khlystov, A., Kos, G. P. A., Tuch, T., Roth, C. and Kreyling, W.: A high flow humidograph for testing the water uptake by ambient aerosol. Atmos. Environ., 34, 4291–4300, 2000.Wang, J. and Martin, S. T.: Satellite characterization of urban aerosols: Importance of including hygroscopicity and mixing state in the retrieval algorithms, J. Geophys. Res., 112, D17203, 2007.

WMO/GAW: Aerosol measurement procedures guidelines and recommendations, GAWRep. 153, World Meteorol. Organ., Geneva, Switzerland. (Available at http://wdca.jrc.it/data/gaw153.pdf), 2003.

Yan, P., Pan, X., Tang, J., Zhou, X., Zhang, R. and Zeng, L.: Hygroscopic growth of aerosol scattering coefficient: A comparative analysis between urban and suburban sites at winter in Beijing, Particuology, 7, 52-60, 2009.

Zieger, P., Fierz-Schmidhauser, R., Gysel, M., Ström, J., Henne, S., Yttri, K., Baltensperger, U., and Weingartner E.: Effects of relative humidity on aerosol light scattering in the Arctic, Atmos. Chem. Phys., 10(8), 3875–3890, doi:10.5194/acp-10-3875-2010, 2010.

Zieger, P., Weingartner, E., Henzing, J., Moerman, M., de Leeuw, G., Mikkilä, J., Ehn, M., Petäjä, T., Clémer, K., van Roozendael, M., Yilmaz, S., Frieβ, U., Irie, H., Wagner, T., Shaiganfar, R., Beirle, S., Apituley, A., Wilson, K., and Baltensperger, U.: Comparison of ambient aerosol extinction coefficients obtained from in-situ, MAX-DOAS and LIDAR measurements at Cabauw, Atmos. Chem. Phys., 11, 2603-2624, 2011.

Zieger, P., Kienast-Sjögren, E., Starace, M., von Bismarck, J., Bukowiecki, N., Baltensperger, U., Wienhold, F., Peter, T., Ruhtz, T., Collaud Coen, M., Vuilleumier, L., Maier, O., Emili, E., Popp, C. and Weingartner E.: Spatial variation of aerosol optical properties around the high-alpine site Jungfraujoch (3580 m a.s.l.), Atmos. Chem. Phys., 12, 7231–7249, doi: 10.5194/acp-12-7231-2012, 2012.

Zieger, P., Fierz-Schmidhauser, R., Weingartner, E. and Baltensperger, U.: Effects of relative humidity on aerosol light scattering: results from different European sites, Atmos. Chem. Phys., 13, 10609-10631, 2013.

Table 1. Mean and standard deviation of single scattering albedo, scattering Ångström exponent, γ parameter, $\gamma_{>65\%}$, $\gamma_{<65\%}$ and scattering enhancement factor at 80% RH for PM_{10} fraction and scattering enhancement factor at 80% RH for PM_1 fraction for the two wind sectors. All the variables refer to 550 nm except the scattering Ångström exponent that has been calculated between 450 and 700 nm.

Sector	SSA	SAE	γ	$\gamma_{>65\%}$	$\gamma_{<65\%}$	f(RH=80%)	f(RH=80%) in PM_1
Anthro-pogenic	0.93±0.03	1.8±0.5	0.4±0.1	0.5±0.2	0.4±0.1	1.8±0.2	1.7±0.2
Marine	0.98±0.02	0.9±0.3	0.7±0.1	0.9±0.2	0.4±0.1	2.2±0.3	2.5±0.6

Table 2. Hygroscopic growth factors reported in the literature for marine environments. The values of f(RH) corresponds to the ratio of the aerosol light scattering coefficients (near 550 nm wavelength) at high RH (85% unless noted: *RH = 82%, **RH=80%) and at dry conditions (RH<40%). All samples were taken with size cut (D_p) of 10 μm unless specifically noted.

Source	Location	Year	f(RH)	Notes
Hegg et al. (1996a)	eastern North Pacific Ocean	1994		No D_p cut
			2.3**	Clean marine
Li-Jones et al. (1998)	Barbados, West Indies	1994	1.8**	Sea salt
Carrico et al. (1998)	Cape Grim, Tasmania	1995	1.98*	Clean marine
McInnes et al. (1998)	Sable Island, Canada	1996		D_p<1 μm
			2.7	Marine
			1.7	Polluted
Kotchenruther et al. (1999)	western North Atlantic Ocean	1996		D_p <4 μm,
			1.81**	"less anthropogenic"
			2.30**	"more anthropogenic"
Carrico et al. (2000)	Sagres, Portugal	1997		D_p <10 μm
			1.69*	Clean
			1.46*	Polluted
				D_p <1 μm
			1.86*	Clean
			1.48*	Polluted
Gassó et al. (2000)	eastern North	1997		D_p < 2.5 μm

	Atlantic Ocean		2.0**	Polluted
			2.5**	Clean
Sheridan et al. (2002)	Indian Ocean	1999		D_p <1 μm
	Indian Ocean (North)		1.55	Polluted
	Indian Ocean (Central)		1.69	Polluted
			2.07	Clean marine
	Southern Hemisphere			
Carrico et al. (2003)	Asia/Pacific region	2001		D_p <10 μm
			2.45*	Marine
			2.24*	Polluted
				D_p <1 μm
			2.95*	Marine
			2.52*	Polluted
Fierz-Schmidhauser et al. (2010b)	Mace Head, Ireland	2009	2.2	Clean
			1.8	Polluted
Zieger et al. (2011)	Cabauw, The Netherlands	2009	3	Maritime
This study	Cape Cod, MA	2012-2013		D_p <10 μm
			2.2**	Clean marine
			1.8**	Anthropogenic
				D_p <1 μm
			2.5**	Clean marine
			1.7**	Anthropogenic

Table 3. Mean and standard deviation of single scattering albedo, scattering Ångström exponent, γ parameter, $\gamma_{>65\%}$, $\gamma_{<65\%}$ and scattering enhancement factor at 80% RH for the five clusters. All the variables refer to PM_{10} unless specifically noted and to 550 nm except the scattering Ångström exponent that has been calculated between 450 and 700 nm.

Cluster	SSA	SAE	γ	$\gamma_{>65\%}$	$\gamma_{<65\%}$	f(RH=80%)	f(RH=80%) in PM_1
1	0.94±0.04	1.9±0.7	0.5±0.2	0.6±0.3	0.4±0.1	1.9±0.3	1.8±0.4
2	0.95±0.04	1.8±0.6	0.5±0.1	0.5±0.2	0.4±0.1	1.9±0.3	1.8±0.3
3	0.92±0.04	1.9±0.5	0.4±0.1	0.6±0.2	0.4±0.1	1.7±0.2	1.6±0.3
4	0.92±0.03	2.1±0.5	0.4±0.1	0.5±0.2	0.4±0.1	1.8±0.2	1.7±0.2
5	0.97±0.03	1.1±0.5	0.7±0.2	0.9±0.2	0.4±0.1	2.1±0.3	2.5±0.6

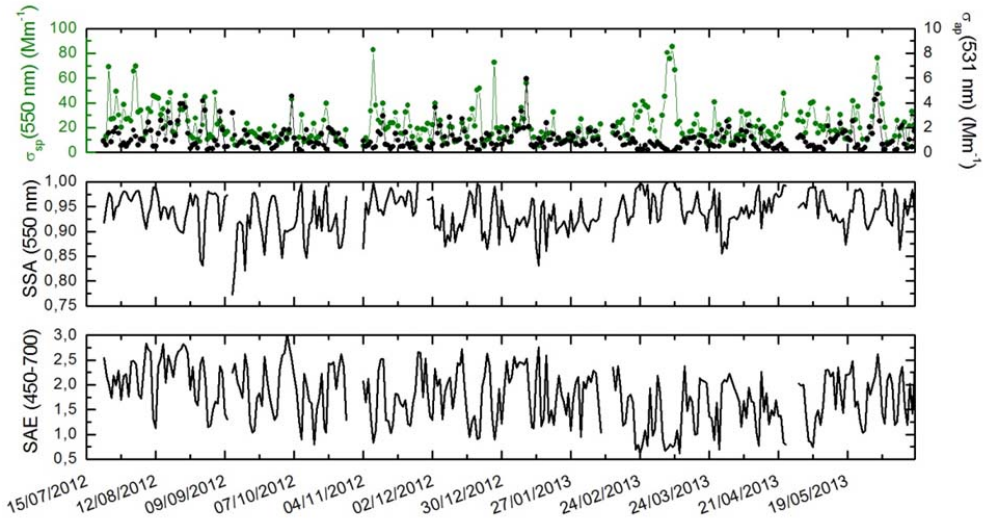

Figure 1. Temporal evolution of the daily dry scattering and absorption coefficients (upper panel), the single scattering albedo (middle panel) and the scattering Ångström exponent (lower panel). All the parameters correspond to the PM_{10} fraction. The date is in the format dd/mm/yyyy.

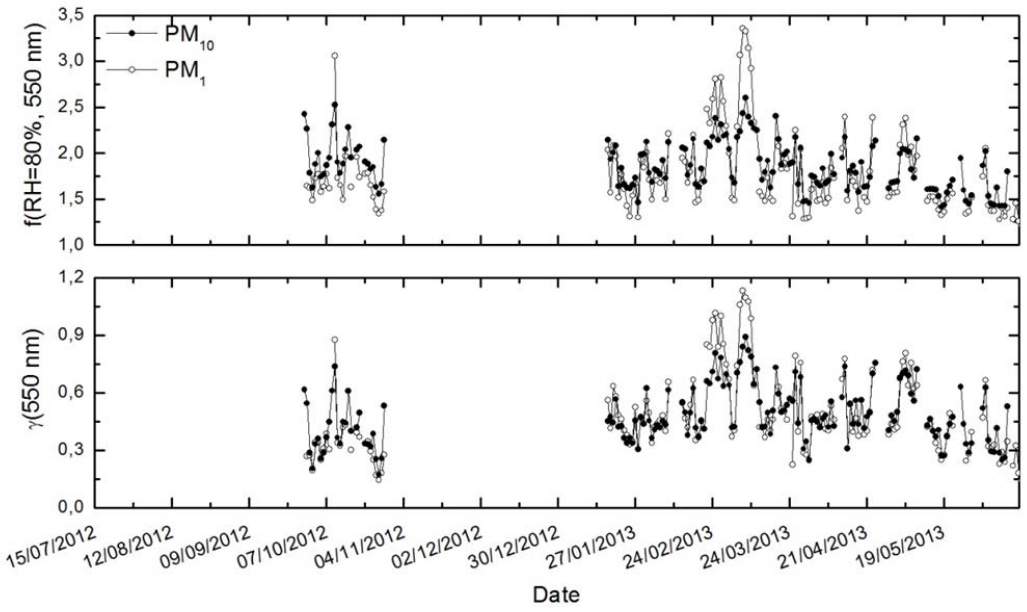

Figure 2. Temporal evolution of the daily scattering enhancement factor at 80% relative humidity (upper panel) and the fit parameter γ (lower panel), for PM_{10} and PM_1 fractions. The date is in the format dd/mm/yyyy.

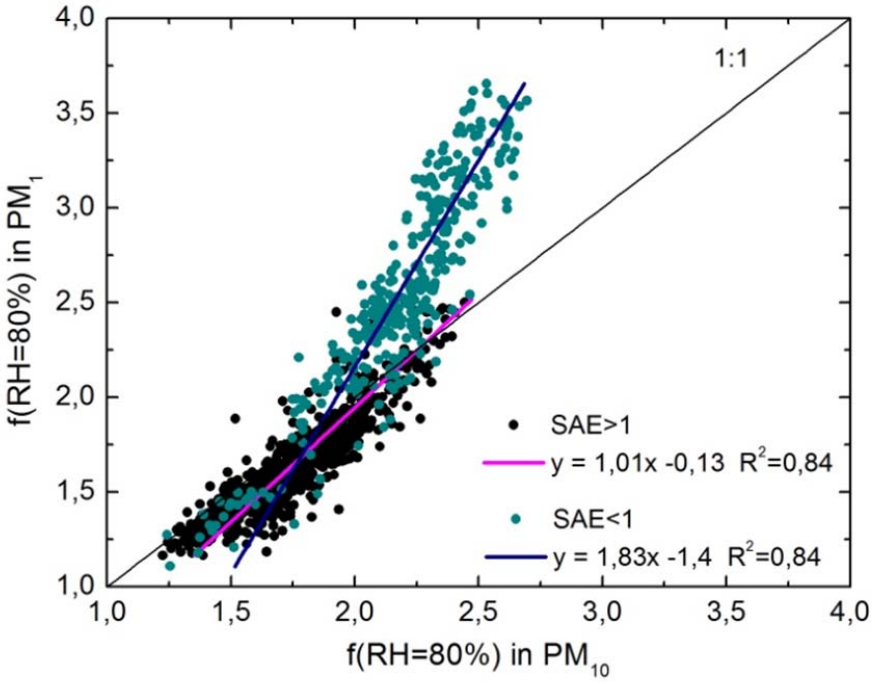

Figure 3. Scatter plot of the hourly average scattering enhancement factors at 80% relative humidity in the PM_1 fraction versus the same parameter in the PM_{10} fraction. Data when the scattering Ångström exponent was below and above 1 were fitted separately.

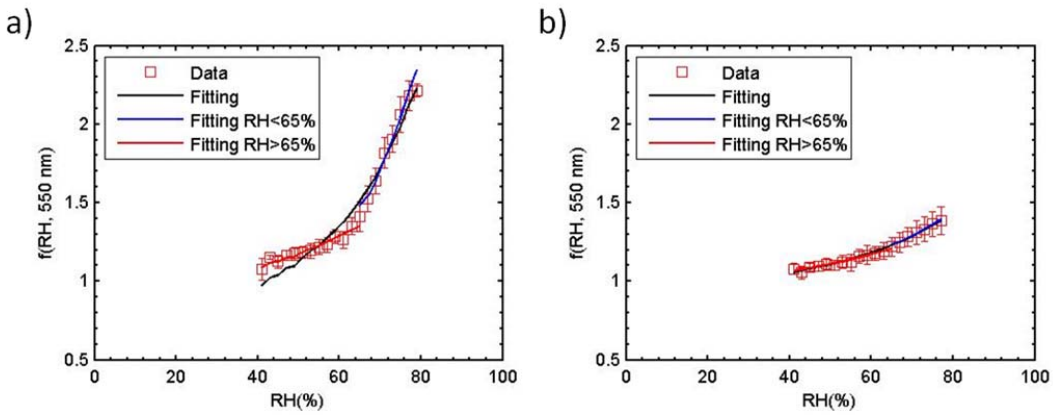

Figure 4. Example humidograms of the scattering enhancement factor, given as daily averages where the error bars represent the standard deviation for the 9th of March (a) and the 31st of May (b). The black line denotes the γ fit for the entire RH range (RH>40%), the blue line denotes the γ fit for RH>65% and the red line the γ fit for the RH<65%.

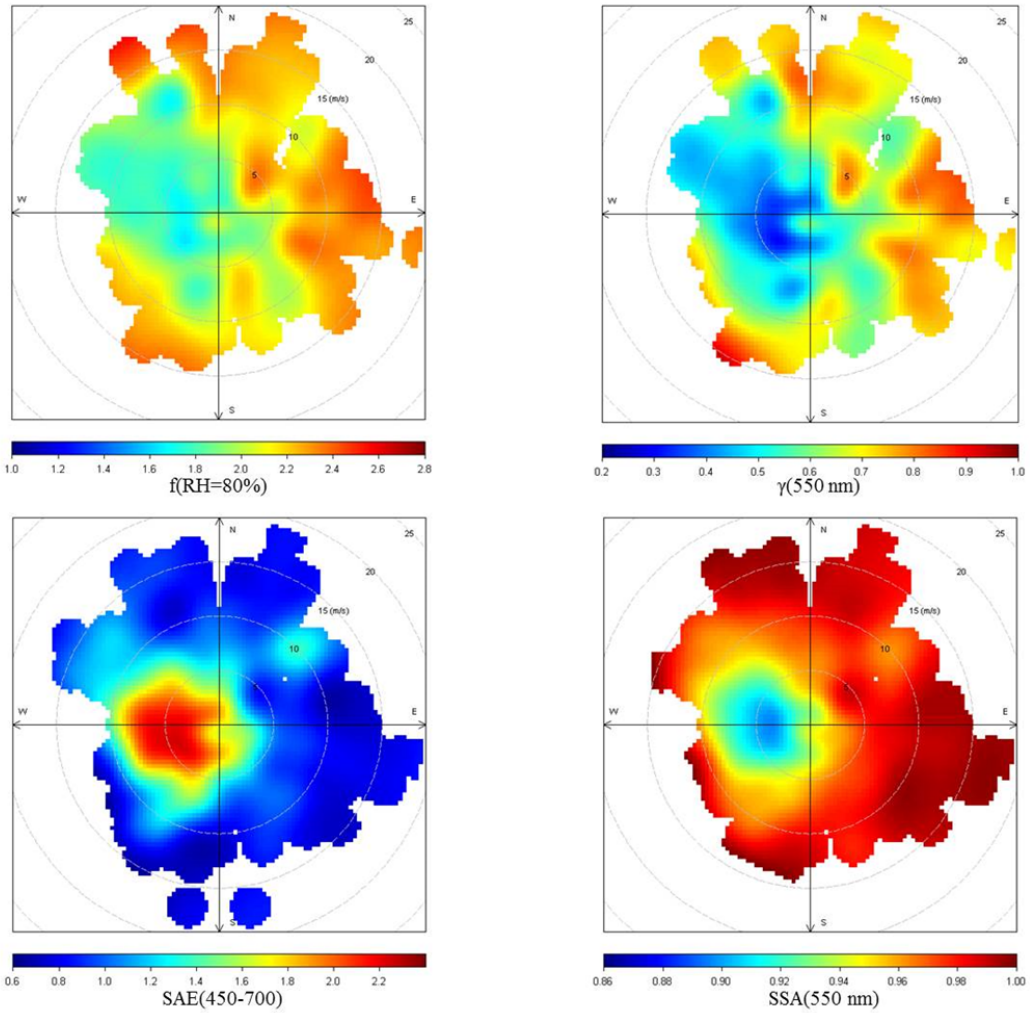

Figure 5. Bivariate plots of the scattering enhancement factor at 80% RH, the γ parameter, single scattering albedo and scattering Ångström exponent as a function of wind speed and direction.

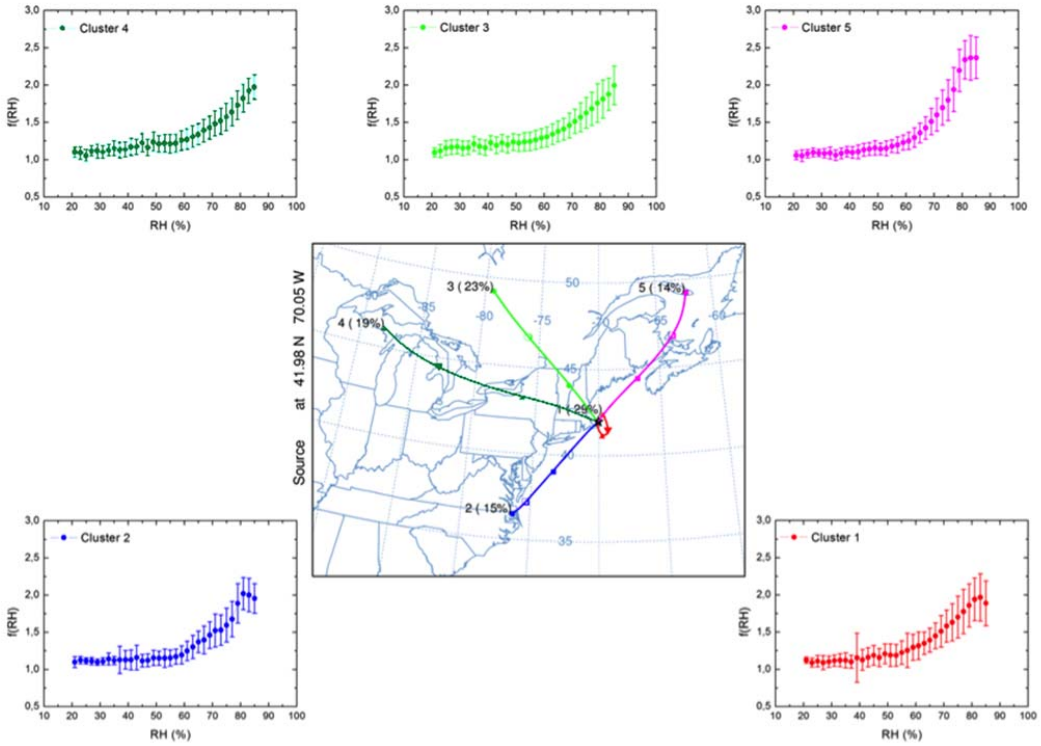

Figure 6. Clusterization of 3-days air masses backtrajectories arriving at Cape Cod at 500 m a.g.l. at 00, 06, 12 and 18 GMT according to the HYSPLIT4 model (central panel) and average humidograms for each cluster. The error bars denote the standard deviation.

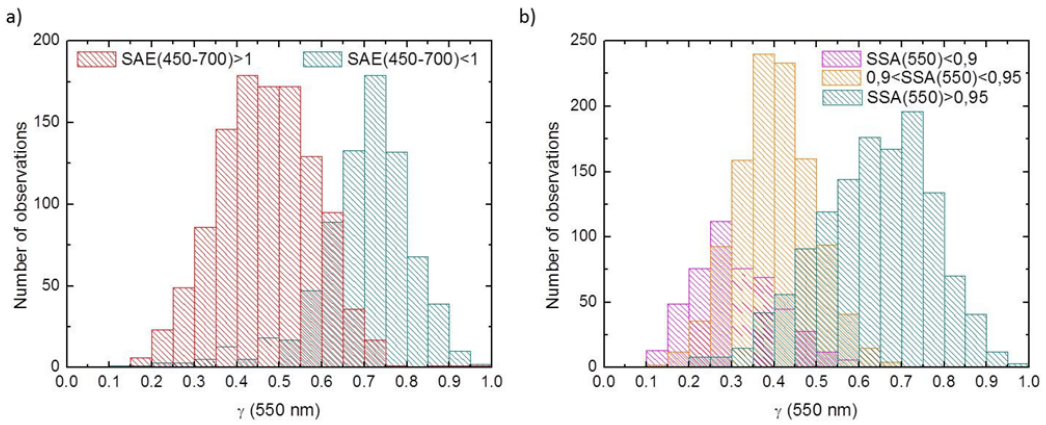

Figure 7. Frequency distribution of the γ parameter for different scattering Ångström exponent (a) and single scattering albedo (b) ranges in the PM_{10} size fraction.

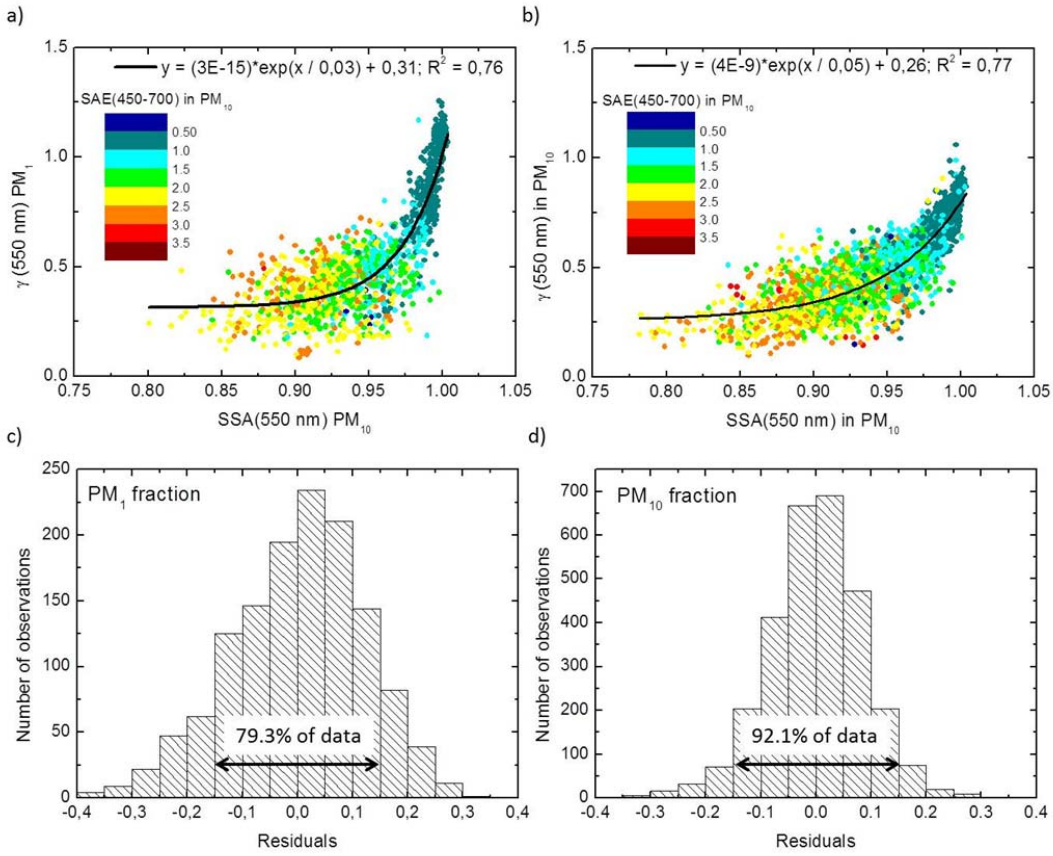

Figure 8. γ parameter in PM_1 (a) and PM_{10} (b) versus the single scattering albedo in PM_{10}. The color code corresponds to the scattering Ångström exponent in PM_{10}. An exponential fit has been added to the plot (black line). The residuals of these regressions are plotted as frequency distributions for PM_1 (c) and PM_{10} (d) size fractions.